Enhanced Hole Mobility and Reliability of Panel Epi-Like Silicon Transistors Using Backside Green Laser Activation

Yu-Ting Lin, Jia-Min Shieh, *Member, IEEE*, and Chih Chen

***Abstract*—The hole mobility and reliability of green continuous-wave laser-crystallized epi-like Si transistors on glass panel substrates were enhanced by source/drain activation by backside green laser irradiation. Green laser energy was scanned uniformly across junctions since the gate structures included no interference, in an attempt to conduct super visible–laser lateral activation. The enhancement was thus explained by the formation of continuous improved epi-like Si microstructures with reduced grain defects and with a barely increased number of interface defects over the entire channel/junction. The hole mobility in such laser-activated devices was as high as 403 $\mathrm{cm^2/V \cdot s}$, which doubles that of thermally activated devices.**

***Index Terms*—Backside green laser activation, continuous-wave (CW) laser crystallization (CLC), epi-like Si transistors.**

I. Introduction

TEMPERATURE constrains the activation of source/drain junctions in several transistors, including panel transistors [1] and integrated-circuit transistors with novel channels and gate dielectrics [2], [3] or shallow junctions [4]–[6]. Accordingly, thermal annealing technologies must continue to advance. Dopant activation by ultraviolet [5], green [6], and near-infrared laser irradiation [7] of source/drain regions has been demonstrated in transistor fabrication. However, laser activation, unlike laser crystallization, produces discontinuities in microstructures across junctions because of variations in the laser energy that is scanned over the device bodies, which are caused by gate structures [8]. With reference to panel applications, thin-film transistors (TFTs) on quartz wafers are reportedly activated by backside excimer laser irradiation and exhibit improved electrical characteristics [9].

Continuous-wave (CW) green laser crystallization (CLC) has attracted substantial interest because it is useful in the formation of epi-like microstructures and the maintenance of crystallized channels with low surface roughness, providing remarkably excellent device reliability and electrical characteristics [10], [11]. Moreover, the fact that the absorption fraction of light energy in transparent substrates decreases substantially as the laser wavelength increases supports the introduction of backside long-wavelength (green) CW laser activation (CLA) in mainstream glass panel displays, reducing laser energy loss and negligibly damaging the interfaces near the substrates.

Manuscript received May 2, 2007; revised June 15, 2007. This work was supported in part by the National Science Council through various grants. The review of this letter was arranged by Editor C.-P. Chang.

Y.-T. Lin and C. Chen are with the Department of Material Science and Engineering, National Chiao Tung University, Hsinchu 30010, Taiwan, R.O.C.

J.-M. Shieh is with the National Nano Device Laboratories, Hsinchu 30078, Taiwan, R.O.C. (e-mail: jmshieh@mail.ndl.org.tw; jmshieh@faculty.nctu.edu.tw).

Color versions of one or more of the figures in this letter are available online at http://ieeexplore.ieee.org.

Digital Object Identifier 10.1109/LED.2007.902984

II. Experiments

Poly-Si channels on Corning Eagle 2000 glass substrates were formed by the green CLC (laser energy of ∼4.2 W) of amorphous silicon islands with thicknesses of 100 nm, which were deposited by plasma-enhanced chemical vapor deposition (PECVD). PECVD SiO_2 grown at 380 °C with a thickness of 100 nm is applied as a gate dielectric. Following the formation of gate structures of Mo/SiO_2, the source and drain regions were doped with B_2H_6 (5.0×10^{14} $\mathrm{cm^{-2}}$ and 40 keV) and activated by rapid thermal annealing (RTA) or backside green CW laser irradiation at 2.1–2.8 W. The sheet resistance of laser (RTA)-activated bare-doped CLC layers was also evaluated using a four-point probe. The stability of fabricated devices with width/length $= 60\ \mu\mathrm{m}/60\ \mu\mathrm{m}$ during hot-carrier stressing (HCS) at gate voltage $(V_g) =$ drain voltage $(V_d) = -20$ V, which condition confirmedly injects hot carriers to deteriorate devices by increasing interface and grain deep-state densities [11], at room temperature was examined. As HCS proceeded, the transfer characteristics (drain current I_d versus V_g) and, therefore, the electrical parameters of the devices were measured periodically during bias stressing [11], [12]. Grain trap-state densities n_{GT} for all TFTs were examined using the field-effect conductance technique [13], where the I_d–V_g curves in the range of 5 to −15 V are taken at numerous temperatures of 25 °C, 50 °C, 75 °C, 100 °C, and 125 °C, respectively.

III. Results and Discussion

As laser activation energy increases, the sheet resistance of the laser-activated layers slowly declines to 1–3 $\mathrm{k\Omega/sq}$, in the same range of that measured in RTA-activated layers [Fig. 1(a)]. Laser activation energy was almost half of the laser crystallization energy. Therefore, laser activation hardly altered the crystallinity and roughness of the CLC epi-like Si channels. Accordingly, the surface roughness of activated layers, i.e., 3.8 nm, was almost identical to that of undoped CLC samples (i.e., 3.7 nm, which is not shown herein). Moreover, the tail-state density of grain traps measured in laser-activated devices, which was closely related to channel crystallinity [14]

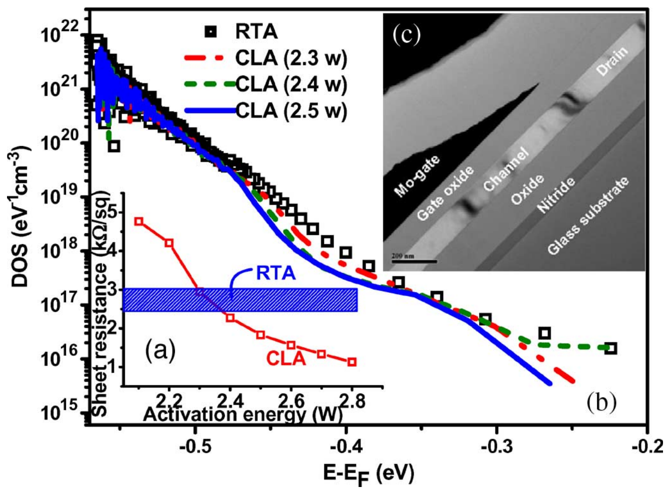

Fig. 1. (a) Sheet resistance of bare CLC layers that were doped with B_2H_6 and activated by RTA and backside green laser irradiation at 2.1–2.8 W. (b) Energy distribution associated with grain trap-state densities in fresh TFTs that were made on CLC poly-Si and activated by RTA and backside green laser irradiation at 2.3–2.5 W. (c) Cross-sectional transmission electron microscopic image of representative laser-activated TFT.

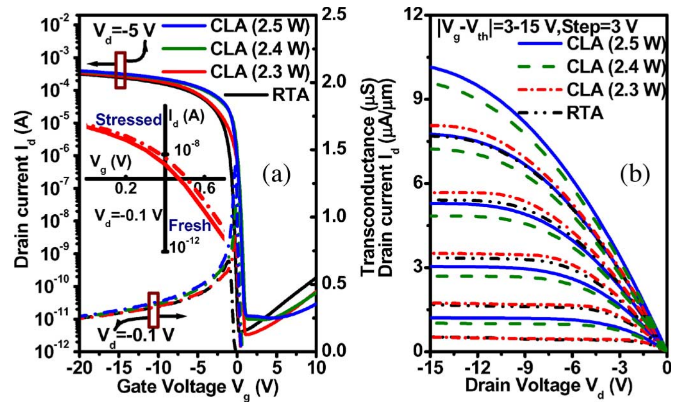

Fig. 2. (a) Transfer characteristics (taken at $V_d = -5$ V) and transconductance curves (taken at $V_d = -0.1$ V). (b) Output characteristics of TFTs that were made on CLC poly-Si and activated by RTA and backside green laser irradiation at 2.3–2.5 W. $I_d - V_g$ curves (taken at $V_d = -0.1$ V) of fresh and stressed devices that were activated by backside green laser irradiation at 2.3 W are also plotted in (a).

n_{GT} at an energetic level E that was far from the Fermi level E_F, $\Delta E = E - E_F = -0.55$ to -0.47 eV, was independent of laser activation energy and identical to that measured in RTA-activated devices [Fig. 1(b)]. Moreover, this laser activation energy was sufficiently high to repair amorphized source/drain regions due to implantation [4] and to recrystallize a few small grains in the channels [15], as indicated by n_{GT} between the middle and the deep energetic levels ($\Delta E = -0.47$ to -0.3 eV), which decreases markedly with laser activation energy [Fig. 1(b)].

As laser activation energy increases, the field-effect mobility μ_{FE} of laser-activated TFTs increases significantly from 255 to 403 $\mathrm{cm}^2/\mathrm{V} \cdot \mathrm{s}$, which is around two times that of RTA-activated TFTs, as revealed by the linear transcondcutance G_m curves, which are plotted in Fig. 2(a). The enhancement in the output drive current [Fig. 2(b)] at $V_d = -15$ V and $V_g = -15$ V was as high as 1.4 times. However, similar changes in sheet resistance (1.5–3 kΩ/sq) by RTA parameters were responsible for no changes in hole mobility and, therefore, temperature-dependent $I_d - V_g$ curves (or n_{GT}) taken in such long-channel TFTs fabricated on CLC or excimer-laser-annealed channels (not shown herein), such that the reduction of contact resistance was ruled out as a major mechanism in hole-mobility enhancement. Under backside green laser irradiation, the gate structures did not influence the distribution of laser energy. Therefore, laser energy was uniformly scanned laterally from channels to source/grain regions and vice versa. Super visible–laser lateral activation consequentially produces continuous epi-like Si microstructures with a reduced number of grain defects across junctions, as indicated by the cross-sectional transmission electron microscopic image in Fig. 1(c), in response to the enhancement.

On such an epi-like poly-Si, interface trap-state densities (at $\Delta E \sim 0$ eV), which are related to channel roughness, influence the subthreshold slope S of fabricated TFTs [11]. The formation of extra interface defects is associated with the enhancement of surface roughness by laser activation, such that increasing the laser activation energy initially reduced S to as low as 91 mV/dec and then slightly increased it to 122 mV/dec (Fig. 3), which value is better than 128 mV/dec for RTA-activated devices. The reversal in threshold voltage V_{th} due to the small increase in the number of interface defects [10], [11] to an extent related to laser activation energy was also observed (Fig. 3). Furthermore, the quality of the interface affects the deep states of the grain traps, such that n_{GT} at a ΔE of above -0.28 eV for devices that were activated at a middle laser activation energy of 2.4 W exceeded that for devices that were activated at a low laser activation energy of 2.3 W [Fig. 1(c)] [11]. However, the greatly improved channel/junction microstructures, which were formed by a relatively high laser activation energy of 2.5 W, were responsible for the fact that the deep states of the grain traps were as low as 8.0×10^{15} eV^{-1} cm^{-3} (at $\Delta E \sim -0.26$ eV).

Improvements in epi-like Si channel/junction microstructures caused by backside laser activation that reduces local electric fields near drain regions, originating in the discontinuity in the microstructures across junctions, were responsible for the decrease in the leakage current in the laser-activated TFTs [Fig. 2(a)] [8].

Fig. 3(a) and (b) plots the transients of V_{th} and S and the degradation of the V_{th} shift (ΔV_{th}) for devices in Fig. 2 during HCS, against laser activation energy and stress time t. After HCS, very small changes in S (ΔS) and V_{th} of 1 mV/dec and 50 mV, respectively, were observed in TFTs that were activated at a low laser energy of 2.3 W, which corresponded to the lowest value (91 mV/dec) of S among all laser-activated devices and a μ_{FE} of 255 $\mathrm{cm}^2/\mathrm{V} \cdot \mathrm{s}$ [Fig. 3(a)]. The worsening of electrical parameters for stressed TFTs activated at a high laser energy of 2.5 W, which corresponded to an S of 122 mV/dec and an extremely high μ_{FE} of 403 $\mathrm{cm}^2/\mathrm{V} \cdot \mathrm{s}$, was deteriorated to 17 mV/dec and -284 mV, respectively. However, these values are better than the 32 mV/dec and -425 mV in RTA-activated TFTs, which exhibited a μ_{FE} of 195 $\mathrm{cm}^2/\mathrm{V} \cdot \mathrm{s}$ and an S of 128 mV/dec.

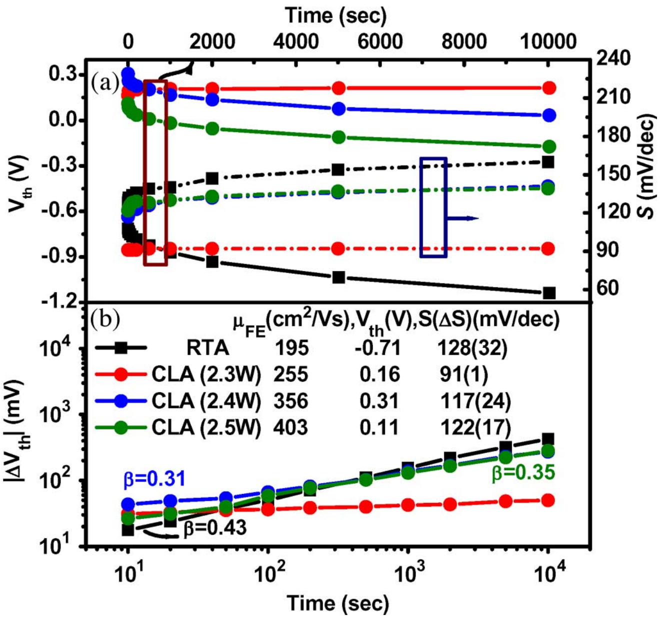

Fig. 3. (a) Transients of threshold voltage and subthreshold slope and (b) degradation of $V_{\rm th}$ of TFTs that were made on CLC poly-Si and activated by RTA and backside green laser irradiation at 2.3–2.5 W during HCS. Electrical parameters for all fresh TFTs are also summarized.

After $\sim$3 h of HCS, a positive rather than a negative shift in $V_{\rm th}$ for the laser-activated device with the lowest S was observed [see the inset of Figs. 2(a) and 3(a)]. This result is attributed to hot-electron trapping near drain junction [16]. The creation of donor-type interface deep states was excluded as a possible mechanism of the positive $V_{\rm th}$ shift [16] because the changes in S (or interface defects) were negligible during HCS [Fig. 3(a)]. The $V_{\rm th}$ degradation for laser-activated devices due to HCS typically follows a power law in time $(\sim t^{\beta})$, with exponents β of less than 0.4, as opposed to $\beta = 0.4{-}0.6$ that is associated with deep-state generation [Fig. 3(b)] [11]. Moreover, HCS hardly changed the tail-state densities of grain traps in highly crystalline laser (RTA)-treated junctions/channels [11], which is consistent with β and reduction percentage of less than 0.3 and 8%, respectively, in $\mu_{\rm FE}$ degradation for both junctions/channels (not shown herein).

Enhanced reliability was irrelevant to relatively small variation in reliability of devices distributed over panels associated with fair uniformity of electrical parameters of $\mu_{\rm FE}$, $V_{\rm th}$, and S of 12%, 0.1 V, and 20%, respectively, and was barely ascribed to the formation of the lightly doped drain structure in such long-channel TFTs by laser-induced lateral diffusion of dopants.

Therefore, the formation of continuous improved epi-like Si microstructures with reduced grain defects and with a barely increased number of interface defects over the entire channel/junction inhibited markedly deep-state generation in laser-treated channels/junctions by bias stressing, in response to the enhancement of the stability of such laser-activated TFTs.

IV. Conclusion

Backside CW green laser irradiation was applied to activate TFTs that were fabricated on CLC epi-like poly-Si. Enhancement in the hole mobility and reliability of such laser-fabricated transistors was demonstrated, and it was explained by the formation of continuous enhanced epi-like Si microstructures with a barely increased number of interface defects over channels/junctions as a result of the lateral activation by uniformly scanned laser energy over the bottom of devices, in the absence of interference by gate structures.

Acknowledgment

The authors would like to thank AU Optronics for the technical assistance.

References

[1] G. K. Giust, T. W. Sigmon, J. B. Boyce, and J. Ho, "High-performance laser-processed polysilicon thin-film transistors," *IEEE Electron Device Lett.*, vol. 20, no. 2, pp. 77–79, Feb. 1999.

[2] Z. Luo, Y. F. Chong, J. Kim, N. Rovedo, B. Greene, S. Panda, T. Sato, J. Holt, D. Chidambarrao, J. Li, R. Davis, A. Madan, A. Turansky, O. Gluschenkov, R. Lindsay, A. Ajmera, J. Lee, S. Mishra, R. Amos, D. Schepis, H. Ng, and K. Rim, "Design of high performance PFETs with strained Si channel and laser anneal," in *IEDM Tech. Dig.*, 2005, pp. 489–492.

[3] Q. Zhang, J. Huang, N. Wu, G. Chen, M. Hong, L. K. Bera, and C. Zhu, "Drive-current enhancement in Ge n-channel MOSFET using laser annealing for source/drain activation," *IEEE Electron Device Lett.*, vol. 27, no. 9, pp. 728–730, Sep. 2006.

[4] R. F. Wood, J. R. Kirkpatrick, and G. E. Giles, "Macroscopic theory of pulsed-laser annealing. II. Dopant diffusion and segregation," *Phys. Rev. B, Condens. Matter*, vol. 23, no. 10, pp. 5555–5569, May 1981.

[5] B. Yu, Y. Wang, H. Wang, Q. Xiang, C. Riccobene, S. Talwar, and M. R. Lin, "70 nm MOSFET with ultra-shallow, abrupt, and super-doped S/D extension implemented by laser thermal process (LTP)," in *IEDM Tech. Dig.*, 1999, pp. 509–512.

[6] R. Murto, K. Jones, M. Rendon, and S. Talwar, "Activation and deactivation studies of laser thermal annealed boron, arsenic, phosphorus, and antimony ultra-shallow abrupt junctions," in *Proc. Int. Conf. Ion Implant. Technol.*, 2000, pp. 155–158.

[7] D. A. Markle, A. M. Hawryluk, and H. J. Jeong, "Apparatus having line source of radiant energy for exposing a substrate," U.S. Patent 6 531 681, Mar. 11, 2003.

[8] D. Z. Peng, T. C. Chang, H. W. Zan, T. Y. Huang, C. Y. Chang, and P. T. Liu, "Reliability of laser-activated low-temperature polycrystalline silicon thin-film transistors," *Appl. Phys. Lett.*, vol. 80, no. 25, pp. 4780–4782, Jun. 2002.

[9] C. W. Lin, C. H. Tseng, T. K. Chang, C. W. Lin, W. T. Wang, and H. C. Cheng, "A novel laser-processed self-aligned gate-overlapped LDD poly-Si TFT," *IEEE Electron Device Lett.*, vol. 23, no. 3, pp. 133–135, Mar. 2002.

[10] Y. T. Lin, C. Chen, J. M. Shieh, Y. J. Lee, C. L. Pan, C. W. Cheng, J. T. Peng, and C. W. Chao, "Trap-state density in continuous-wave laser-crystallized single-grain-like silicon transistors," *Appl. Phys. Lett.*, vol. 88, no. 23, p. 233 511, Jun. 2006.

[11] Y. T. Lin, C. Chen, J. M. Shieh, and C. L. Pan, "Stability of continuous-wave laser-crystallized epi-like silicon transistors," *Appl. Phys. Lett.*, vol. 90, no. 7, p. 073 508, Feb. 2007.

[12] K. S. Karim, A. Nathan, M. Hack, and W. I. Milne, "Drain-bias dependence of threshold voltage stability of amorphous silicon TFTs," *IEEE Electron Device Lett.*, vol. 25, no. 4, pp. 188–190, Apr. 2004.

[13] G. Fortunato and P. Migliorato, "Determination of gap state density in polycrystalline silicon by field-effect conductance," *Appl. Phys. Lett.*, vol. 49, no. 16, pp. 1025–1027, Oct. 1986.

[14] M. Miyasaka and J. Stoemenos, "Excimer laser annealing of amorphous and solid-phase-crystallized silicon films," *J. Appl. Phys.*, vol. 86, no. 10, pp. 5556–5565, Nov. 1999.

[15] K. Y. Choi and M. K. Han, "Two-step annealed polycrystalline silicon thin-film transistors," *J. Appl. Phys.*, vol. 80, no. 3, pp. 1883–1890, Aug. 1996.

[16] N. A. Hastas, C. A. Dimitriadis, J. Brini, and G. Kamarinos, "Hot-carrier-induced degradation in short p-channel nonhydrogenated polysilicon thin-film transistors," *IEEE Trans. Electron Devices*, vol. 49, no. 9, pp. 1552–1557, Sep. 2002.